In Silico Pharmacology (2021) 9:41
https://doi.org/10.1007/s40203-021-00101-1

ORIGINAL RESEARCH

In silico analysis of echinocandins binding to the main proteases of coronaviruses PEDV (3CL^{pro}) and SARS-CoV-2 (M^{pro})

Gérard Vergoten[1] · **Christian Bailly**[2]

Received: 28 May 2021 / Accepted: 25 June 2021
© The Author(s), under exclusive licence to Springer-Verlag GmbH Germany, part of Springer Nature 2021

Abstract

The porcine epidemic diarrhea virus (PEDV) and severe acute respiratory syndrome coronavirus 2 (SARS-CoV-2) are two highly pathogenic viruses causing tremendous damages to the swine and human populations, respectively. Vaccines are available to prevent contamination and to limit dissemination of these two coronaviruses, but efficient and widely affordable treatments are needed. Recently, four natural products targeting the 3C-like protease (3CL^{pro}) of PEDV and inhibiting replication of the virus in vitro have been identified: tomatidine, epigallocatechin-3-gallate, buddlejasaponin IVb and pneumocandin B0. We have evaluated the interaction of these compounds with 3CL^{pro} of PEDV and with the structurally similar main protease (M^{pro}) of SARS-CoV-2. The molecular docking analysis indicated that the echinocandin-type lipopeptide pneumocandin B0 can generate much more stable complexes with both proteases compared to tomatidine. The empirical energy of interaction (ΔE) calculated with pneumocandin B0 bound to M^{pro} is extremely high, comparable to that measured with known antiviral drugs. Pneumocandin B0 and its analogue capsofungin appeared a little less adapted to interact with 3CL^{pro} compared to M^{pro}. In contrast, the antifungal drug micafungin bearing an unfused tricyclic side chain, emerges as a better ligand of 3CL^{pro} of PEDV compared to M^{pro} of SARS-CoV-2, based on our calculations. Collectively, the analysis underlines the benefit of echinocandin-type antifungal drugs as potential inhibitors of PEDV and SARS-CoV-2 main proteases. These clinically important antifungal natural products deserve further studies as antiviral agents.

Keywords Echinocandins · Main protease · Molecular modelling · PEDV · SARS-CoV-2

Abbreviations

3CL^{pro}	Coronavirus 3C-like protease of PEDV
M^{pro}	Main protease of SARS-CoV-2
PNB0	Pneumocandin B0

Introduction

Coronaviruses are a family of enveloped, single-stranded RNA viruses. This genus includes a wide range of important human and animal pathogens, such as the porcine epidemic diarrhea virus (PEDV), Middle East respiratory syndrome coronavirus (MERS-CoV) and severe acute respiratory syndrome coronavirus 1 and 2 (SARS-CoV-1 and -2). Vaccines are now available to reduce the spread of SARS-CoV-2 and to limit the pandemic outbreak of coronavirus disease 2019 (COVID-19). Vaccines are also used to prevent and control PEDV infections (Won et al. 2020; Li et al. 2020a) but more efficient and novel approaches are still needed to combat porcine epidemic diarrhea. This highly contagious intestinal disease has led to substantial economic losses in many countries and is a great threat to the swine industry worldwide (Jung et al. 2020; Russell et al. 2020). Similarly, efficient anti-COVID-19 vaccines are available to prevent the disease and limit viral dissemination, but there is no treatment to eradicate the virus and its mutants. Mass vaccination campaigns are taking places in many countries, but the crusade against COVID-19 pandemic, which is currently impacting every country in the world, remains a priority and a challenge (Madkaikar et al. 2021).

In recent years, different small molecules active against PEDV have been identified, including several natural products such as the isoflavonoid puerarin (Wu et al. 2020, 2021), the polyphenol epigallocatechin-3-gallate (EGCG)

✉ Christian Bailly
christian.bailly@oncowitan.com

[1] Faculté de Pharmacie, Inserm, INFINITE-U1286, Institut de Chimie Pharmaceutique Albert Lespagnol (ICPAL), University of Lille, 3 rue du Professeur Laguesse, BP-83, 59006 Lille, France

[2] OncoWitan, 59290 Lille, Wasquehal, France

Published online: 01 July 2021

(Huan et al. 2021), the alkaloid tomatidine (hereafter designated TD) (Wang et al. 2020a) and the flavonoids quercetin and quercetin 7-rhamnoside (Choi et al. 2009; Li et al. 2020b), to cite only a few examples. One of the most frequently targeted protein of PEDV is the coronavirus 3C-like protease ($3CL^{pro}$), which has a conserved structure and plays a key role in the viral replication process (St John et al. 2016; Ye et al. 2016). Small molecules selectively targeting $3CL^{pro}$ are actively searched (Shi et al. 2018; Ye et al. 2020). Both quercetin and TD were found to inhibit $3CL^{pro}$ and to markedly reduce PEDV attachment and entry into cells (Huan et al. 2021; Wang et al. 2020a). TD has been found to block of 3CL protease activity in PEDV-infected cells and the compound has revealed antiviral activities in vitro against other viruses, notably the transmissible gastroenteritis virus (TGEV), porcine reproductive and respiratory syndrome virus (PRRSV), encephalo-myocarditis virus (EMCV) and Seneca virus A (SVA) in vitro. This steroidal alkaloid was discovered in the frame of a drug screening campaign using a specific library of 911 natural products tested for their anti-PEDV activity in cells. Four compounds have emerged from the primary cell-based screening: TD, EGCG, the triterpene saponin buddlejasaponin IVb (BJ-IVb) and the antifungal cyclic-lipopetide pneumocandin B0 (PNB0) (Fig. 1). These four natural products were found to markedly inhibit infection of Vero cells with PEDV in a dose-dependent manner, while showing little or no direct cytotoxic effects. Both TD and PNB0 potently inhibited the viral infection (IC_{50} = 3.45 and 3.48 mM respectively) whereas BJ-IVb and EGCG were slightly less active (IC_{50} = 8.14 and 8.76 mM respectively) (Wang et al. 2020a). Based on its favorable selectivity, Wang and coworkers selected TD to characterize further its anti-PEDV activity and in particular its capacity to block viral replication in cells. Moreover, TD was shown to bind to a purified recombinant

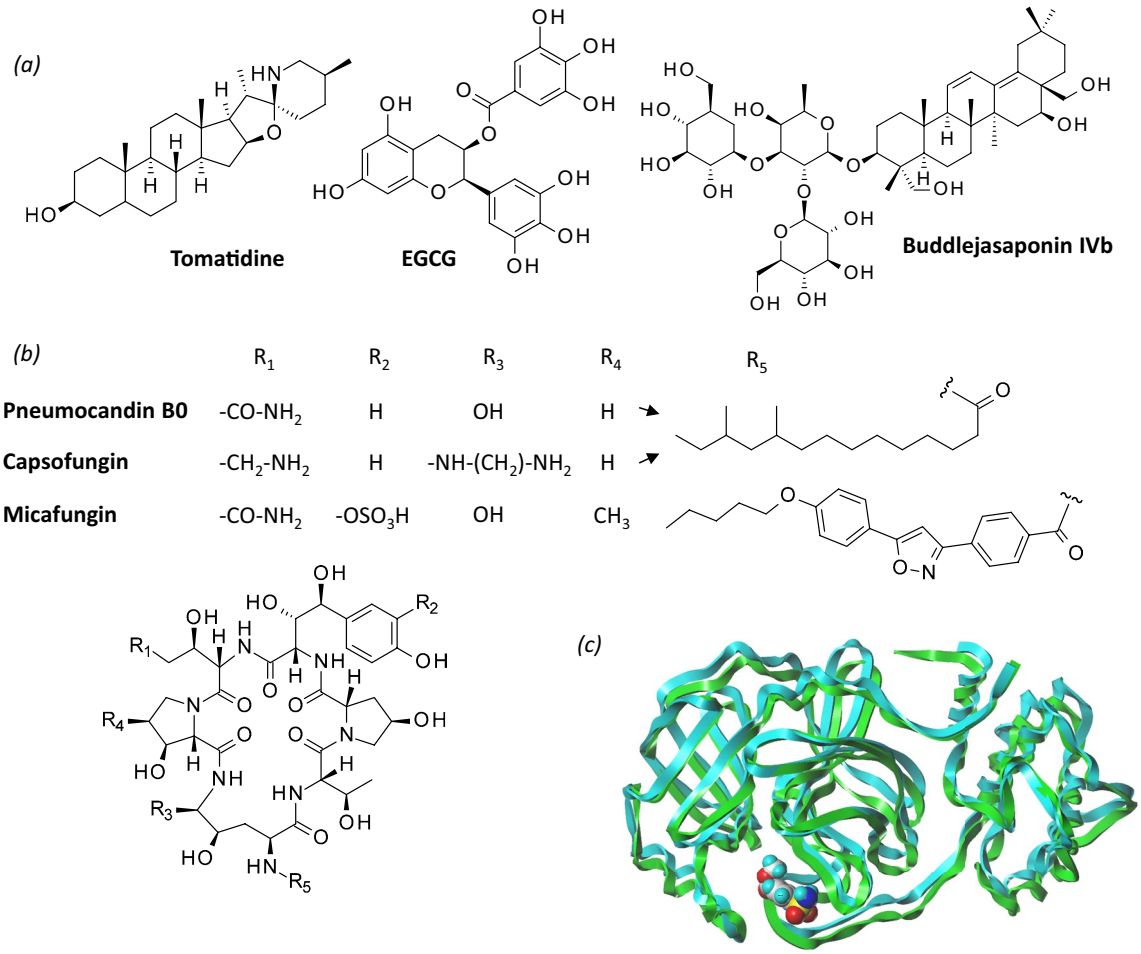

Fig. 1 **a** Structures of tomatidine (TD, CID: 65576), epigallocatechin-3-gallate (EGCG, CID: 65064) and buddlejasaponin IVb (BJ-IVb, CID: 91758420). **b** Structures of the three echinocandin derivatives pneumocandin B0 (PNB0, CID: 72475), micafungin (477468) et capsofungin (CID: 2826718). **c** Superimposed ribbon structures of the two viral proteases: M^{pro} of SARS-CoV-2 with its co-crystalized ligand (PDB code: 5R80) and $3CL^{pro}$ of PEDV (PDB code: 4XFQ), in *green* and *cyan*, respectively

form of PEDV-3CL^{pro} (Kd = 2.78 µM) and a molecular modeling analysis suggested that the compound can bind to the active site of the enzyme. This elegant study concluded that TD inhibits PEDV replication mainly by targeting 3CL protease (Wang et al. 2020a).

This study prompted us to investigate further the potential binding of all four compounds TD, PNB0, BJ-IVb and EGCG to the PEDV 3C-like protease, taking advantage of the crystallographic structure of the protein (Ye et al. 2016). The interactions of the four compounds with protease 3CL^{pro} were analyzed and compared. In parallel, we investigated the binding of these molecules to the main protease (M^{pro}) of SARS-CoV-2 because these two coronavirus main proteases present a highly conserved structure and catalytic mechanism (Fig. 1c). We reasoned that the four inhibitors of PEDV-3CL^{pro} might be able to bind to SARS-CoV-2 M^{pro}, as observed for example, with the dipeptidyl inhibitor GC376 targeting both proteases (Wang et al. 2020b). The primary objective of our computational study was to define and compare the mode of binding of the four compounds to both 3CL^{pro} (PEDV) and M^{pro} (SARS-CoV-2). Our in silico analysis indicates that PNB0 has the capacity to form much more stable complexes than TD with the two proteases. This work raises the hypothesis that the antifungal drug pneumocandin B0 (PNB0) can interfere with the activity of the viral proteases, suggesting therefore that other member of the echinocandins family of anti-fungal drugs might also be able to interact with these proteins (Fig. 2). The hypothesis was tested in silico with the related drugs capsofungin and micafungin, structurally close to PNB0 (Fig. 1b).

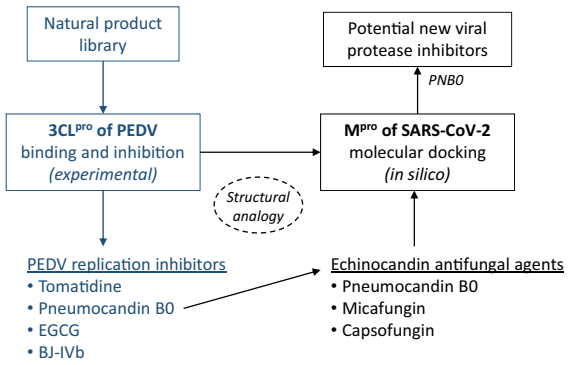

Fig. 2 Schematic diagram of the study design. Screening of a natural product library has identified four inhibitors of PEDV replication in cells targeting protease 3CL^{pro}, including pneumocandin B0 (Wang et al. 2020a). We took advantage of the structural analogy between 3CL^{pro} of PEDV and M^{pro} of SARS-CoV-2 to search for potential viral protease inhibitors, through the analysis of echinocandin-type antifungal agents

Table 1 Calculated potential energy of interaction (ΔE, kcal/mol) and free energy of hydration (ΔG, kcal/mol) for the interaction of the two viral proteases with the indicated natural products

Compounds	3CL^{pro} of PEDV		M^{pro} of SARS-CoV-2	
	ΔE	ΔG	ΔE	ΔG
TD	−48.3	−21.6	−44.3	−19.1
EGCG	−80.0	−20.0	−89.0	−26.3
BJ-IVb	−68.5	−28.4	−82.7	−26.0
PNB0	−80.7	−26.1	−97.8	−45.0
Capsofungin	−81.1	−46.3	−95.1	−31.1
Micafungin	−93.5	−41.4	−81.5	−30.3

TD tomatidine, *EGCG* epigallocatechin-3-gallate, *BJ-IVb* buddlejasaponin IVb, *PNB0* pneumocandin B0

Methods

In silico molecular docking procedure

The tridimensional structures of the SARS-CoV-2 main protease in complex with a small molecule inhibitor (Z18197050) and the PEDV 3C-like protease were retrieved from the Protein Data Bank (www.rcsb.org) under the PDB codes 5R80 and 4XFQ, respectively (Douangamath et al. 2020; Ye et al. 2016). Docking experiments were performed with the GOLD software (GOLD 5.3 release, Cambridge Crystallographic Data Centre, Cambridge, UK). Before starting the docking procedure, the structure of the ligands has been optimized using a classical Monte Carlo conformational searching procedure as described in the BOSS software (Jorgensen et al. 2004).

With the 5R80 structure, based on shape complementarity criteria, the binding site for the ligands has been defined around amino acid residue Met165 (binding site for the ligand Z18197050). Given the important structural similarities between the two proteases, the position of the binding site is comparable in the 4XFQ structure and is centered on amino acid residue Glu187. Shape complementarity and geometry considerations are in favor of a docking grid centered in the volume defined by this amino acid. Within the binding site, side chains of specific amino acids have been considered as fully flexible. The flexible amino acids are (i) His41, Met49, Tyr54, Cys145, His164, Met165, Glu166, Phe181, Val186 and Asp187 for structure 5R80 and (ii) His41, Thr47, Tyr53, Cys144, Gln163, Leu164, Glu165, Glu185, Asp186 and Glu187 for structure 4XFQ. The ligand is always defined as flexible during the docking procedure. Up to 100 poses that are energetically reasonable were kept while searching for the correct binding mode of the ligand. The decision to keep a trial pose is based on ranked poses, using the PLP fitness scoring function [which is the default in GOLD version 5.3 used here (Jones

et al. 1997)]. The same procedure was used to establish molecular models for all compounds listed in Tables 1 and 2. The empirical potential energy of interaction ΔE for the ranked complexes is evaluated using the simple expression ΔE(interaction) = E(complex)—(E(protein) + E(ligand)). For that purpose, the spectroscopic empirical potential energy function SPASIBA and the corresponding parameters were used (Vergoten et al. 2003; Lagant et al. 2004). Free energies of hydration (ΔG) were estimated using the MM/GBSA model in Monte Carlo simulations within the BOSS software (Jorgensen et al. 2004). The stability of the receptor-ligand complex is evaluated through the empirical potential energy of interaction (Vergoten et al. 2003; Lagant et al. 2004). The molecular mechanics/generalized born surface area (MM/GBSA) procedure was used to evaluate free energies of hydration (Jorgensen et al. 2004) [within the Boss program (Jorgensen and Tirado-Rives 2005)], in relation with aqueous solubility (Zafar and Reynisson 2016). Molecular graphics and analysis were performed using Discovery Studio Visualizer, Biovia 2020 (Dassault Systèmes BIOVIA Discovery Studio Visualizer 2020, San Diego, Dassault Systèmes, 2020).

The two most widely used methods to investigate protein–ligand stability and affinity are molecular dynamics (MD) and Monte Carlo (MC) simulations. Both methods use an empirical force field to control the total energy (MC, energy minimization) and forces (MD, Newton equations of motion). To use MD simulations confidently, a force field parameterized for dynamical properties is required. The development of a reliable and accurate force field for the conformational analysis is a concern. It requires accuracy of the force field over the whole potential surface, rather than in the region of the global minimum (Homans 1990). The most used academic force fields (CHARMM, AMBER, GROMOS) do not exhibit the required vibrational spectroscopic quality. Determination of normal modes on a minimized protein structure using the above force fields can result in imaginary wavenumbers corresponding to maxima in the potential energy (transition states, mainly due to inadequate barriers to internal rotation). The spectroscopic SPASIBA force field has been specifically developed to provide refined empirical molecular mechanics force field parameters, as described in other studies (Vergoten et al. 2003; Meziane-Tani et al. 2006). For this reason, we preferred to use MC simulations rather than MD which requires a substantial increase in computer time to achieve the same level of convergence (Jorgensen and Tirado-Rives, 1996).

Table 2 Calculated potential energy of interaction (ΔE, kcal/mol) and free energy of hydration (ΔG, kcal/mol) for the interaction of the different compounds with M^{pro} of SARS-CoV-2

	CID#[b]	DE	DG
Pneumocandin B0	72475	−97.81	−45.00
Capsofungin	2826718	−95.10	−31.10
Micafungin	477468	−81.85	−30.30
Glecaprevir[a]	66828839	−96.50	−41.30
Pibrentasvir	58301952	−96.50	−34.50
Paritaprevir	45110509	−87.30	−17.00
Elbasvir	71661251	−85.31	−26.40
Zanamivir	60855	−83.10	−25.10
Darunavir	213039	−82.00	−20.40
Ritonavir	3926922	−81.80	−21.00
Lopinavir	92727	−79.40	−30.60
Grazoprevir	44603531	−76.70	−23.00
Ombistavir	54767916	−76.05	−27.20
Delavirdine	5625	−78.80	−18.00
Velpatasvir	67683363	−73.80	−27.50
Sofosbuvir	45375808	−73.80	−24.20
Remdesivir	121304016	−73.10	−21.75
Daclatasvir	25154714	−72.60	−26.30
Simeprevir	24873435	−66.60	−29.20
Nelfinavir	64143	−66.60	−24.30
Ledipasvir	67505836	−65.00	−25.40
Molnupiravir	145996610	−63.50	−14.80
Tenofovir	464205	−52.00	−21.30
Entecavir	135398508	-47.30	−17.30

[a]Data for the reference antiviral compounds (Vergoten and Bailly 2021)

[b]Compound Identity number, as defined in PubChem (https://pubchem.ncbi.nlm.nih.gov)

Results

The structures of the studied compounds are shown in Fig. 1. Tomatidine is a steroidal alkaloid found in unripe (green) tomatoes, generally derived from its glycoside a-tomatine (Friedman 2013). Epigallocatechin-3-gallate (EGCG) is a well-known green tea catechin with marked anti-inflammatory and antiviral properties (Chourasia et al. 2021). Buddlejasaponin IVb (BJ-IVb) is a triterpene saponin isolated from *Clinopodium chinense* (Benth.) O. Kuntze (Zeng et al. 2016) and from the aerial part of *Pleurospermum kamtschaticum* Auct. (Jung et al. 2005). Pneumocandin B0 (PNB0) is an antifungal lipohexapeptide of the echinocandin family, inhibitor of 1,3-β-glucan synthase of fungal cell (Li et al. 2018). Capsofungin and micafungin, two structural analogues of PNB0, are approved drugs used to treat diverse fungal infections (Hashemian et al. 2020; Taormina et al. 2021). Pneumocandin B0, capsofungin and micafungin belong to the echinocandin family of antifungal agents, which are largely used to treat aspergillosis, candidiasis and other fungal diseases (Mroczyńska and Brillowska-Dąbrowska 2020; Hüttel 2021).

To investigate the interaction of these compounds with the 3CL^{pro} of PEDV, we used the crystal structure of the protease (PDB: 4XFQ) and performed a molecular docking analysis to identify the preferred drug binding site. The interaction site is centered on residue Glu187 (which superimposes well with the known M^{pro} binding site of SARS-CoV-2, vide infra). Molecular models were constructed with each ligand and we calculated the empirical energy of interaction (ΔE) and free energy of hydration (ΔG), as reported in Table 1. Surprisingly, we found large variations in ΔE values between compounds. Both PNB0 and EGCG appear to form very stable complexes with 3CL^{pro}, much more favorable than the complex formed with BJ-IVb. The ΔE value calculated with TD is only 60% of the value calculated with PNB0. Representative binding models are shown in Fig. 3 for TD and PNB0. At first sight, TD seems to fit well into the drug binding cavity but the molecular contacts between the drug and the protein surface are weaker and fewer than with PNB0. The TD-3CL^{pro} complex is stabilized by different van der Waals contacts and (p)alkyl interactions but there is a single hydrogen bond between the protein and the phenolic OH group of TD (Fig. 3f). On the opposite, multiple H-bonds can be identified between PNB0 and 3CL^{pro} (Fig. 3c). The compound strongly interacts with the protein, mainly via its hydrophilic cyclic peptide moiety whereas the appended lipophilic dimethyl-myristoyl chain essentially points toward the outside of the protein. Similar models were obtained with compounds EGCG and BJ-IVb. The polyphenol EGCG can form equally stable complexes with M^{pro} compared to PNB0, whereas the triterpene saponin BJ-IVb appears to be much less adapted to interact with the protease. To sum up this first part, the four ligands rank in the order PNB0, EGCG > BJ-IVb > TD for their capacity to form complexes with 3CL^{pro}.

The prominent capacity of PNB0 to bind to 3CL^{pro} of PEDV, as determined experimentally (Wang et al. 2020a) and via our computational analysis, prompted us to include two structural analogues, the approved drugs capsofungin and micafungin. We found little difference between PNB0 and capsofungin for binding to 3CL^{pro}, in contrast to micafungin which presents a higher binding capacity (Table 1). Capsofungin bears the same dimethyl-myristoyl chain (R_5 in Fig. 1b) as PNB0 but has an additional amino side chain (R_3) apparently little contributing to the protein interaction (but reinforcing the water solubility of the compound). The unfused tricyclic side chain (R_5) of micafungin lies into a groove adjacent to the binding site, allowing additional contacts with 3CL^{pro}. The model in Fig. 4a shows the

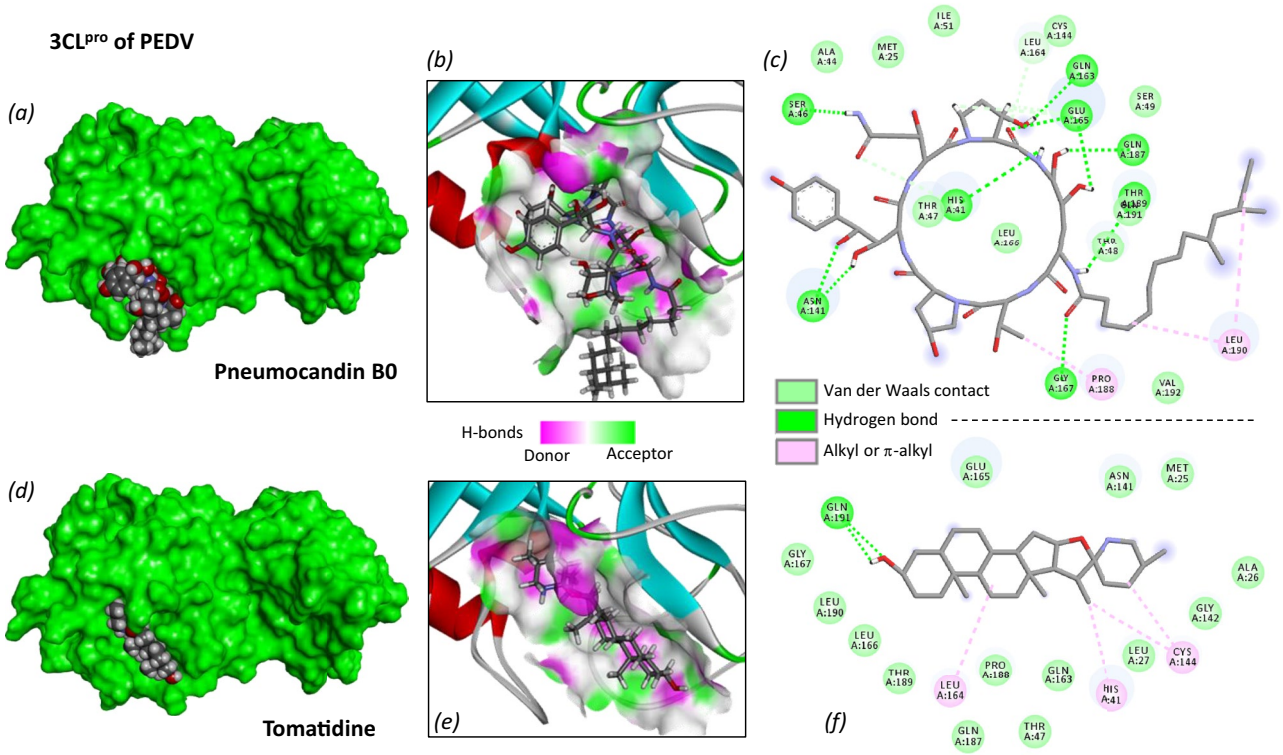

Fig. 3 Molecular models of pneumocandin B0 and tomatidine bound to 3CL^{pro} of PEDV. Panels **a** and **d** show the ligand bound to the active site cavity of the protein (green). Panels **b** and **e** show a detailed view of the compound in the binding site, with the H-bond donor and acceptor groups available within the cavity. Panels **c** and **f** refer to the binding map contacts for each ligand, with the indicated color code

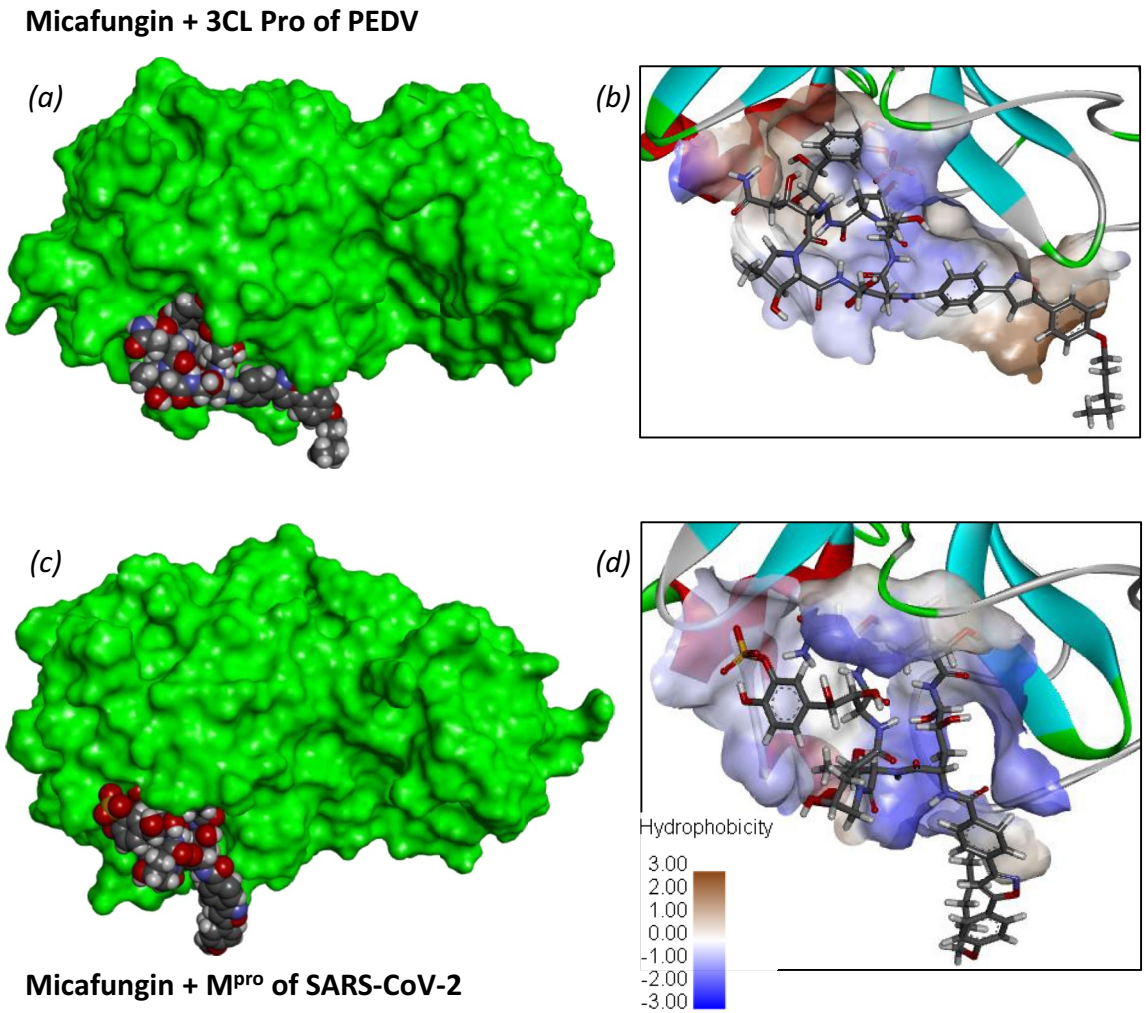

Fig. 4 Models of micafungin bound to the two proteases (**a**, **c**). Close-up view of the ligand bound to the active site, with the hydrophobic/hydrophilic zones colored in brown and blue, respectively. Note the divergent orientation of the unfused tri-aromatic side chain of micafungin between the two models. The side chain interacts with the protein edge in the case of $3CL^{pro}$ whereas is essentially free in the case of M^{pro}

position of the phenyl-oxazole-phenyl unit of micafungin, interacting with the edge of the $3CL^{pro}$ protein. Compared to PNB0, there are additional van der Waals and p-alkyl contacts with micafungin side chain, accounting for its superior capacity to bind to $3CL^{pro}$ compared to PNB0.

Next, considering the large structural similarity between the main proteases of PEDV and SARS-CoV-2 (Fig. 1c), we performed similar docking analyses with the protein M^{pro}, based on its known crystallographic structure (PDB: 5R80). In this case, there is a small molecule fragment in the crystal structure occupying a pocket around residues His164/Met165/Asp187 (Douangamath et al. 2020). This ligand was removed prior to evaluating the capacity of each natural product to bind to this site. The calculated ΔE and ΔG values (Table 1) indicate that the lipopeptide PNB0 has the highest capacity to form stable complexes with the protease compared to the three other ligands tested. The four compounds rank in the order PNB0 > EGCG > BJ-IVb > TD for their capacity to form complexes with M^{pro} of SARS-CoV-2. The difference of ΔE values between TD and PNB0 is huge. The tomato alkaloid TD is clearly not well adapted to interact with the viral protease. In sharp contrast, PNB0 emerges has a potential high-affinity ligand, at least from an in silico perspective. Representative models of PNB0-M^{pro} complexes are shown in Fig. 5 and similar models were obtained with the other compounds. PNB0 seems to be extremely well adapted to bind to the active site of the SARS-CoV-2 main protease. Multiple interaction sites between the natural product and the protein can be identified, including several H-bonds. The hydrophilic peptide ring of PNB0 fits perfectly into the protein cavity. In particular, the (3*R*)-hydroxy-glutamine portion of PNB0 interacts with residues Thr24 and

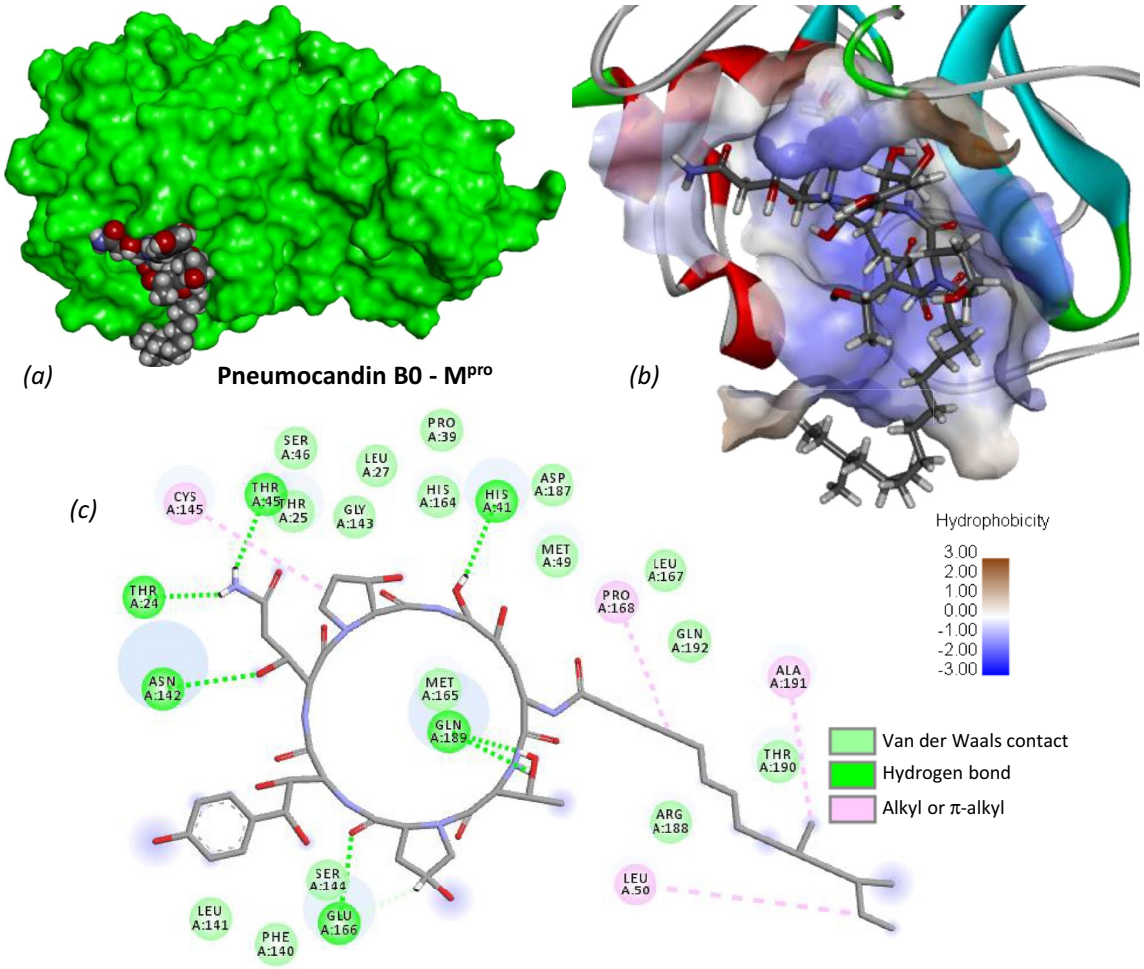

Fig. 5 Molecular models of pneumocandin B0 bound to M^{pro} of SARS-CoV-2. **a** The ligand bound to the protein active site. **b** A close-up view of the compound in the binding site, with the hydrophobic/hydrophilic zones colored in brown and blue, respectively. **c** Binding map contact, with the indicated color code

Asn142 of M^{pro} and the (2S,3R)-threonine residue of PNB0 interacts with Gln189 of the protein (Fig. 5c). Compared to $3CL^{pro}$, in this case the lipophilic side chain of PNB0 is a little bit more implicated in the interaction with M^{pro} but the essential of the complex stability is provided by the cyclic peptide moiety.

Both the empirical energy of interaction (ΔE) and free energy of hydration (ΔG) are extremely high for the PNB0-M^{pro} complex. In a recent study, we have computed the interaction of more than 30 references compounds, mainly antiviral drugs, with the M^{pro} protein using the same molecular docking procedure (Vergoten and Bailly 2021). The best ligands were the two anti-hepatitis C virus drugs glecaprevir and pibrentasvir. It is remarkable to see that the ΔE and ΔG values calculated with PNB0 are on the same level as those measured with these two potent antiviral drugs, well superior to the values calculated with all the other antiviral agents (Table 2). Several studies have reported that glecaprevir and pibrentasvir are high-affinity inhibitors of SARS-CoV-2 main protease (Shamsi et al. 2020; Bahadur Gurung et al. 2020; Chtita et al. 2021; Bhat et al. 2021). Our computational analysis suggests that the antifungal compound pneumocandin B0 is equally well suited to interact with this key viral protease.

The remarkable capacity of PNB0 to bind to the M^{pro} protein prompted us to extend our analysis to the structurally related compounds capsofungin and micafungin. As in the case of $3CL^{pro}$, we found little difference between PNB0 and capsofungin for binding to M^{pro}. They can form equally stable complexes with the SARS-Cov-2 protease (Table 1). In contrast, the unfused tricyclic side chain of micafungin now appears as a negative element for binding to M^{pro}, whereas it was a positive element for binding to $3CL^{pro}$ (Fig. 4). In the case of M^{pro}, the bulky aromatic side chain essentially lies outside of the protein cavity and does not contribute to the drug binding process. In contrast, as mentioned above,

this aromatic side chain was found to reinforce drug binding to $3CL^{pro}$.

Discussion

Drugs active against coronaviruses are actively searched. Natural products are largely considered as a source of bioactive molecules and several compounds have shown promise for the inhibition of coronavirus in humans (Mani et al. 2020). In this context, our study was built on the recent discovery by Wang and workers of the capacity of the four natural products to inhibit the $3CL^{pro}$ of PEDV (Wang et al. 2020a). They identified tomatidine, epigallocatechin-3-gallate, buddlejasaponin IVb, and pneumocandin B0 as $3CL^{pro}$ inhibitors and focused their study on tomatidine which was found to inhibit PEDV replication in cells. They demonstrated that TD could bind to the PEDV protease, likely representing a major target for steroidal alkaloid. Here, we have extended the study of these natural products to the binding to $3CL^{pro}$ of PEDV and the structurally similar main protease (M^{pro}) of SARS-Cov-2. Our study failed to confirm that $3CL^{pro}$ can represent a major target for TD. This alkaloid displays activities against several viruses, including the porcine epidemic diarrhea virus (PEDV) (Wang et al. 2020a, b), dengue virus (Diosa-Toro et al. 2019) and chikungunya virus (Troost et al. 2020). TD is likely a multitargeted agent.

The main point of our work is the identification of echinocandin-type drugs as potential ligands of main proteases of both PEDV and SARS-Cov-2. We show that pneumocandin B0 displays a very high capacity of interaction with M^{pro} of SARS-Cov-2, comparable to that measured with the reference antiviral drugs glecaprevir and pibrentasvir. Pneumocandin B0 is a biosynthetic precursor of capsofungin (Chen et al. 2015) which appears to be equally able to bind to M^{pro} according to our calculations. A repurposing of this drug for COVID-19 has been proposed recently (Khadka et al. 2020). Both pneumocandin B0 and capsofungin emerge as good potential binder to M^{pro} of SARS-Cov-2, less efficient against $3CL^{pro}$ of PEDV. The calculated empirical energies of interaction (ΔE) are about 15% lower with $3CL^{pro}$ compared to M^{pro} (Table 1). Interestingly, we found that the related drug micafungin is extremely well suited to bind to the PEDV protease, surpassing its two analogues when we compare the ΔE values. Micafungin is an antifungal drug of great value, largely used to treat neonatal candidiasis (Taormina et al. 2021) and to prevent invasive fungal infections in cancer patients (Park et al. 2019; Marena et al. 2021). Recently, this member of the echinocandin family has also been shown to inhibit Dengue virus infection (Chen et al. 2021) and has revealed activities against chikungunya virus (Ho et al. 2018) and enterovirus 71 (EV71) which is the main pathogen of the hand, foot, and mouth disease (Kim et al. 2016). EV71 bears a 3C protease essential to promote the replication of the virus (Wen et al. 2020). This specific protease could be a primary target for micafungin. The drug is used in COVID-19 patients to combat opportunistic candidiasis (Salehi et al. 2020; Sari et al. 2021). Very recently, micafungin was identified as an inhibitor of 3CL protease of SARS-Cov-2 in vitro and its capacity to bind to the monomeric form of 3CLpro was characterized using molecular dynamics simulations (Mody et al. 2021). Our own molecular docking approach supports these observations and provides additional information, via the comparison of the echinocandin binding to the two proteases M^{pro} of SARS-Cov-2 and $3CL^{pro}$ of PEDV, and preliminary structure-binding information.

At the experimental level, pneumocandin B0 has been found to bind to PEDV-$3CL^{pro}$ (Kd = 2.78 µM) (Wang et al. 2020a; b) whereas micafungin was found to inhibit M^{pro} of SARS-Cov-2 (IC_{50} = 47.6 mM) (Mody et al. 2021). Our in silico analysis offers novel perspective with these compounds, anticipating a good capacity of pneumocandin B0 to inhibit M^{pro} of SARS-Cov-2 and a major effect of micafungin on PEDV-$3CL^{pro}$. In broader terms, the different studies provide a solid rational to investigate further the antiviral proteases properties of the various echinocandins. This clinically important class of non-ribosomal antifungal lipopeptides should be further considered to target coronavirus proteases and to combat various viral infections.

Many potential inhibitors of the main protease of SARS-Cov-2 have been identified through computational methods and/or virtual screening approaches (Li et al. 2020c; Zhai et al. 2021). Our study adds two members of the echinocandin class of antifungal drugs as potential inhibitors of M^{pro}. An experimental validation of this hypothesis is now ongoing.

Author contributions GV investigation; visualization; software. CB conceptualization; visualization; writing—original draft; writing—review and editing.

Funding This research did not receive any specific grant from funding agencies in the public, commercial, or not-for-profit sectors.

Declarations

Conflict of interest The authors declare no conflict of interest associated with this publication and there has been no significant financial support for this work that could have influenced its outcome.

References

Bahadur Gurung A, Ajmal Ali M, Lee J, Abul Farah M, Mashay Al-Anazi K (2020) Structure-based virtual screening of phytochemicals and repurposing of FDA approved antiviral drugs

unravels lead molecules as potential inhibitors of coronavirus 3C-like protease enzyme. J King Saud Univ Sci 32:2845–2853
Bhat ZA, Chitara D, Iqbal J, Sanjeev BS, Madhumalar A (2021) Targeting allosteric pockets of SARS-CoV-2 main protease M(pro). J Biomol Struct Dyn. https://doi.org/10.1080/07391102.2021.1891141
Chen L, Yue Q, Li Y, Niu X, Xiang M, Wang W, Bills GF, Liu X, An Z (2015) Engineering of Glarea lozoyensis for exclusive production of the pneumocandin B0 precursor of the antifungal drug caspofungin acetate. Appl Environ Microbiol 81:1550–1558
Chen YC, Lu JW, Yeh CT, Lin TY, Liu FC, Ho YJ (2021) Micafungin inhibits dengue virus infection through the disruption of virus binding, entry, and stability. Pharmaceuticals (basel) 14:338
Choi HJ, Kim JH, Lee CH, Ahn YJ, Song JH, Baek SH, Kwon DH (2009) Antiviral activity of quercetin 7-rhamnoside against porcine epidemic diarrhea virus. Antivir Res 81:77–81
Chourasia M, Koppula PR, Battu A, Ouseph MM, Singh AK (2021) EGCG, a green tea catechin, as a potential therapeutic agent for symptomatic and asymptomatic SARS-CoV-2 infection. Molecules 26:1200
Chtita S, Belhassan A, Aouidate A, Belaidi S, Bouachrine M, Lakhlifi T (2021) Discovery of potent SARS-CoV-2 inhibitors from approved antiviral drugs via docking and virtual screening. Comb Chem High Throughput Screen 24:441–454
Diosa-Toro M, Troost B, van de Pol D, Heberle AM, Urcuqui-Inchima S, Thedieck K, Smit JM (2019) Tomatidine, a novel antiviral compound towards dengue virus. Antivir Res 161:90–99
Douangamath A, Fearon D, Gehrtz P, Krojer T, Lukacik P, Owen CD, Resnick E, Strain-Damerell C, Aimon A, Ábrányi-Balogh P, Brandão-Neto J, Carbery A, Davison G, Dias A, Downes TD, Dunnett L, Fairhead M, Firth JD, Jones SP, Keeley A, Keserü GM, Klein HF, Martin MP, Noble MEM, O'Brien P, Powell A, Reddi RN, Skyner R, Snee M, Waring MJ, Wild C, London N, von Delft F, Walsh MA (2020) Crystallographic and electrophilic fragment screening of the SARS-CoV-2 main protease. Nat Commun 11:5047
Friedman M (2013) Anticarcinogenic, cardioprotective, and other health benefits of tomato compounds lycopene, alpha-tomatine, and tomatidine in pure form and in fresh and processed tomatoes. J Agric Food Chem 61:9534–9550
Hashemian SM, Farhadi T, Velayati AA (2020) Caspofungin: a review of its characteristics, activity, and use in intensive care units. Expert Rev Anti Infect Ther 18:1213–1220
Ho YJ, Liu FC, Yeh CT, Yang CM, Lin CC, Lin TY, Hsieh PS, Hu MK, Gong Z, Lu JW (2018) Micafungin is a novel anti-viral agent of chikungunya virus through multiple mechanisms. Antivir Res 159:134–142
Homans SW (1990) A molecular mechanical force field for the conformational analysis of oligosaccharides: comparison of theoretical and crystal structures of Man alpha 1–3Man beta 1–4GlcNAc. Biochemistry 29:9110–9118
Huan C, Xu W, Ni B, Guo T, Pan H, Jiang L, Li L, Yao J, Gao S (2021) Epigallocatechin-3-gallate, the main polyphenol in green tea, inhibits porcine epidemic diarrhea virus in vitro. Front Pharmacol 12:628526
Hüttel W (2021) Echinocandins: structural diversity, biosynthesis, and development of antimycotics. Appl Microbiol Biotechnol 105:55–66
Jones G, Willett P, Glen RC, Leach AR, Taylor R (1997) Development and validation of a genetic algorithm for flexible docking. J Mol Biol 267:727–748
Jorgensen WL, Tirado-Rives J (1996) Monte Carlo versus molecular dynamics for conformational sampling. J Phys Chem 100:14508–14513
Jorgensen WL, Tirado-Rives J (2005) Molecular modeling of organic and biomolecular systems using BOSS and MCPRO. J Comput Chem 26:1689–1700
Jorgensen WL, Ulmschneider JP, Tirado-Rives J (2004) Free energies of hydration from a generalized Born model and an ALL-atom force field. J Phys Chem B 108:16264–16270
Jung HJ, Kim SG, Nam JH, Park KK, Chung WY, Kim WB, Lee KT, Won JH, Choi JW, Park HJ (2005) Isolation of saponins with the inhibitory effect on nitric oxide, prostaglandin E2 and tumor necrosis factor-alpha production from Pleurospermum kamtschaticum. Biol Pharm Bull 28:1668–1671
Jung K, Saif LJ, Wang Q (2020) Porcine epidemic diarrhea virus (PEDV): an update on etiology, transmission, pathogenesis, and prevention and control. Virus Res 286:198045
Khadka S, Yuchi A, Shrestha DB, Budhathoki P, Al-Subari SMM, Ziad Alhouzani TM, Anwar Butt I (2020) Repurposing drugs for COVID-19: an approach for treatment in the pandemic. Altern Ther Health Med 26:100–107
Kim C, Kang H, Kim DE, Song JH, Choi M, Kang M, Lee K, Kim HS, Shin JS, Jeong H, Jung S, Han SB, Kim JH, Ko HJ, Lee CK, Kim M, Cho S (2016) Antiviral activity of micafungin against enterovirus 71. Virol J 13:99
Lagant P, Nolde D, Stote R, Vergoten G, Karplus M (2004) Increasing normal modes analysis accuracy: the SPASIBA spectroscopic force field introduced into the CHARMM program. J Phys Chem A 108:4019–4029
Li Y, Lan N, Xu L, Yue Q (2018) Biosynthesis of pneumocandin lipopeptides and perspectives for its production and related echinocandins. Appl Microbiol Biotechnol 102:9881–9891
Li Z, Cao H, Cheng Y, Zhang X, Zeng W, Sun Y, Chen S, He Q, Han H (2020a) Inhibition of porcine epidemic diarrhea virus replication and viral 3C-like protease by quercetin. Int J Mol Sci 21:8095
Li Z, Li X, Huang YY, Wu Y, Liu R, Zhou L, Lin Y, Wu D, Zhang L, Liu H, Xu X, Yu K, Zhang Y, Cui J, Zhan CG, Wang X, Luo HB (2020b) Identify potent SARS-CoV-2 main protease inhibitors via accelerated free energy perturbation-based virtual screening of existing drugs. Proc Natl Acad Sci USA 117:27381–27387
Li Z, Ma Z, Li Y, Gao S, Xiao S (2020c) Porcine epidemic diarrhea virus: Molecular mechanisms of attenuation and vaccines. Microb Pathog 149:104553
Madkaikar M, Gupta N, Yadav RM, Bargir UA (2021) India's crusade against COVID-19. Nat Immunol 22:258–259
Mani JS, Johnson JB, Steel JC, Broszczak DA, Neilsen PM, Walsh KB, Naiker M (2020) Natural product-derived phytochemicals as potential agents against coronaviruses: a review. Virus Res 284:197989
Marena GD, Dos Santos Ramos MA, Bauab TM, Chorilli M (2021) Biological properties and analytical methods for micafungin: a critical review. Crit Rev Anal Chem 51:312–328
Meziane-Tani M, Lagant P, Semmoud A, Vergoten G (2006) The SPASIBA force field for chondroitin sulfate: vibrational analysis of D-glucuronic and *N*-acetyl-D-galactosamine 4-sulfate sodium salts. J Phys Chem A 110:11359–11370
Mody V, Ho J, Wills S, Mawri A, Lawson L, Ebert MCCJC, Fortin GM, Rayalam S, Taval S (2021) Identification of 3-chymotrypsin like protease (3CLPro) inhibitors as potential anti-SARS-CoV-2 agents. Commun Biol 4:93
Mroczyńska M, Brillowska-Dąbrowska A (2020) Review on current status of echinocandins use. Antibiotics (basel) 9:227
Park H, Youk J, Shin DY, Hong J, Kim I, Kim NJ, Lee JO, Bang SM, Yoon SS, Park WB, Koh Y (2019) Micafungin prophylaxis for acute leukemia patients undergoing induction chemotherapy. BMC Cancer 19:358
Russell LE, Polo J, Meeker D (2020) The Canadian 2014 porcine epidemic diarrhoea virus outbreak: Important risk factors that were

not considered in the epidemiological investigation could change the conclusions. Transbound Emerg Dis 67:1101–1112

Salehi M, Ahmadikia K, Mahmoudi S, Kalantari S, Jamalimoghadamsiahkali S, Izadi A, Kord M, Dehghan Manshadi SA, Seifi A, Ghiasvand F, Khajavirad N, Ebrahimi S, Koohfar A, Boekhout T, Khodavaisy S (2020) Oropharyngeal candidiasis in hospitalised COVID-19 patients from Iran: species identification and antifungal susceptibility pattern. Mycoses 63:771–778

Sari AP, Darnindro N, Yohanes A, Mokoagow MI (2021) Role of tocilizumab for concomitant systemic fungal infection in severe COVID-19 patient: case report. Medicine (baltimore) 100:e25173

Shamsi A, Mohammad T, Anwar S, AlAjmi MF, Hussain A, Rehman MT, Islam A, Hassan MI (2020) Glecaprevir and Maraviroc are high-affinity inhibitors of SARS-CoV-2 main protease: possible implication in COVID-19 therapy. Biosci Rep 40:BSR20201256

Shi Y, Lei Y, Ye G, Sun L, Fang L, Xiao S, Fu ZF, Yin P, Song Y, Peng G (2018) Identification of two antiviral inhibitors targeting 3C-like serine/3C-like protease of porcine reproductive and respiratory syndrome virus and porcine epidemic diarrhea virus. Vet Microbiol 213:114–122

St John SE, Anson BJ, Mesecar AD (2016) X-ray structure and inhibition of 3C-like protease from porcine epidemic diarrhea virus. Sci Rep 6:25961

Taormina G, Gopinath R, Moore J, Yasinskaya Y, Colangelo P, Reynolds K, Nambiar S (2021) A regulatory review approach for evaluation of micafungin for treatment of neonatal candidiasis. Clin Infect Dis. https://doi.org/10.1093/cid/ciab025

Troost B, Mulder LM, Diosa-Toro M, van de Pol D, Rodenhuis-Zybert IA, Smit JM (2020) Tomatidine, a natural steroidal alkaloid shows antiviral activity towards chikungunya virus in vitro. Sci Rep 10:6364

Vergoten G, Bailly C (2021) Interaction of the renin inhibitor aliskiren with the SARS-CoV-2 main protease: a computational approach **(unpublished data)**

Vergoten G, Mazur I, Lagant P, Michalski JC, Zanetta JP (2003) The SPASIBA force field as an essential tool for studying the structure and dynamics of saccharides. Biochimie 85:65–73

Wang P, Bai J, Liu X, Wang M, Wang X, Jiang P (2020a) Tomatidine inhibits porcine epidemic diarrhea virus replication by targeting 3CL protease. Vet Res 51:136

Wang YC, Yang WH, Yang CS, Hou MH, Tsai CL, Chou YZ, Hung MC, Chen Y (2020b) Structural basis of SARS-CoV-2 main protease inhibition by a broad-spectrum anti-coronaviral drug. Am J Cancer Res 10:2535–2545

Wen W, Qi Z, Wang J (2020) The function and mechanism of enterovirus 71 (EV71) 3C protease. Curr Microbiol 77:1968–1975

Won H, Lim J, Noh YH, Yoon I, Yoo HS (2020) Efficacy of porcine epidemic diarrhea vaccines: a systematic review and meta-analysis. Vaccines (basel) 8:642

Wu M, Zhang Q, Yi D, Wu T, Chen H, Guo S, Li S, Ji C, Wang L, Zhao D, Hou Y, Wu G (2020) Quantitative proteomic analysis reveals antiviral and anti-inflammatory effects of puerarin in piglets infected with porcine epidemic diarrhea virus. Front Immunol 11:169

Wu M, Yi D, Zhang Q, Wu T, Yu K, Peng M, Wang L, Zhao D, Hou Y, Wu G (2021) Puerarin enhances intestinal function in piglets infected with porcine epidemic diarrhea virus. Sci Rep 11:6552

Ye G, Deng F, Shen Z, Luo R, Zhao L, Xiao S, Fu ZF, Peng G (2016) Structural basis for the dimerization and substrate recognition specificity of porcine epidemic diarrhea virus 3C-like protease. Virology 494:225–235

Ye G, Wang X, Tong X, Shi Y, Fu ZF, Peng G (2020) Structural basis for inhibiting porcine epidemic diarrhea virus replication with the 3C-like protease inhibitor GC376. Viruses 2020(12):240

Zafar A, Reynisson J (2016) Hydration free energy as a molecular descriptor in drug design: a feasibility study. Mol Inform 35:207–214

Zeng B, Liu GD, Zhang BB, Wang SS, Ma R, Zhong BS, He BQ, Liang Y, Wu FH (2016) A new triterpenoid saponin from *Clinopodium chinense* (Benth.) O. Kuntze Nat Prod Res 30:1001–1008

Zhai T, Zhang F, Haider S, Kraut D, Huang Z (2021) An integrated computational and experimental approach to identifying inhibitors for SARS-CoV-2 3CL protease. Front Mol Biosci 8:661424

Publisher's Note Springer Nature remains neutral with regard to jurisdictional claims in published maps and institutional affiliations.